IAEA
INTERNATIONAL ATOMIC ENERGY AGENCY

21st IAEA Fusion Energy Conference

Chengdu, China, 16-21 October 2006

IAEA-CN-149 / EX / 2-1

Study of Turbulence and Radial Electric Field Transitions in ASDEX Upgrade using Doppler Reflectometry

G.D.Conway[1], J.Schirmer[1], C.Angioni[1], J.C.Fuchs[1], R.Dux[1], F.Jenko[1], E.Holzhauer[2], S.Klenge[2], B.Kurzan[1], C.Maggi[1], A.G.Peeters[1], E.Poli[1], M.Reich[1], F.Ryter[1], B.Scott[1], W.Suttrop[1], C.Tröster[1], E.Wolfrum[1], H.Zohm[1] and the ASDEX Upgrade Team

[1]Max-Planck-Institut für Plasmaphysik, EURATOM Association, D-85748 Garching, Germany
[2]Institut für Plasmaforschung, Pfaffenwaldring 31, D-70569 Stuttgart, Germany

Study of Turbulence and Radial Electric Field Transitions in ASDEX Upgrade using Doppler Reflectometry

G.D.Conway[1], J.Schirmer[1], C.Angioni[1], J.C.Fuchs[1], R.Dux[1], F.Jenko[1], E.Holzhauer[2], S.Klenge[2], B.Kurzan[1], C.Maggi[1], A.G.Peeters[1], E.Poli[1], M.Reich[1], F.Ryter[1], B.Scott[1], W.Suttrop[1], C.Tröster[1], E.Wolfrum[1], H.Zohm[1] and the ASDEX Upgrade Team

[1]Max-Planck-Institut für Plasmaphysik, EURATOM Association, D-85748 Garching, Germany
[2]Institut für Plasmaforschung, Pfaffenwaldring 31, D-70569 Stuttgart, Germany
e-mail contact of main author: Garrard.Conway@ipp.mpg.de

Abstract
The radial electric field, E_r, is a crucial factor in the performance of magnetically confined plasmas and on density turbulence. On ASDEX Upgrade Doppler reflectometry has been developed for direct measurement of E_r profiles, its radial shear and its fluctuations. In the plasma edge the E_r radial profile shows the narrow negative well coinciding with the steep pedestal pressure gradient whose depth scales with the plasma confinement: from typically -5 kV m^{-1} in ohmic and L-mode conditions to -30 kV m^{-1} in H-modes, to over -50 kV m^{-1} in improved H-modes. The structure of the edge E_r profile is notably robust, but the core E_r of non-NBI heated discharges when increasing collisionality reverses from positive to negative with a transition in the dominant turbulence from TEM to ITG. Coherent E_r fluctuations with geodesic acoustic mode (GAM) behaviour are observed in the plasma edge, coinciding with region of high plasma vorticity and E_r shearing. GAMs are not detected in the core or in H-mode. The mode has the expected frequency scaling of sound speed over major radius but with additional dependency on plasma elongation and q.

1. Introduction

The radial electric field, E_r, is an important factor in the performance of magnetically confined plasmas and on density fluctuations and turbulence. In fusion plasmas E_r is generally inferred from spectroscopic measurements of impurities, or from potential measurements using heavy ion beam probes. Each technique has its drawbacks, such as limited temporal or spatial resolution, expensive or complicated hardware, and sophisticated analysis procedure. On ASDEX Upgrade microwave Doppler reflectometry has been developed for the direct measurement of E_r profiles, its radial shear and its fluctuations. By deliberately tilting a standard fluctuation reflectometer to the plasma cutoff (i.e. non-normal incidence angle) a hybrid diagnostic is created with the wavenumber sensitivity of microwave scattering and the excellent radial localization of reflectometry. The received signal is Doppler frequency shifted f_D directly proportional to the density turbulence rotation velocity in the plasma $E \times B$ frame, $u_\perp = v_{E\times B} + v_{ph}$, and an intensity determined by the turbulence amplitude. This offers several measurement applications:
(1) When $v_{E\times B} \gg v_{ph}$ (which is the normal situation) then there is a direct measure of E_r with exceptional spatial and/or temporal resolution [1–4],
(2) With the addition of a second channel the instantaneous E_r shear plus turbulence correlation properties are measurable [5],
(3) When $v_{E\times B} \lesssim v_{ph}$ then one can study the turbulence properties via the phase velocity [6],
(4) Since $\tilde{E}_r \rightarrow \tilde{v}_{E\times B} \rightarrow \tilde{f}_D$ this gives direct access to long wavelength E_r fluctuations [7],
(5) By varying the tilt angle, and hence the probed wavenumber (defined by Bragg eqn.), the turbulence wavenumber spectrum can be measured from the intensity of the Doppler peak [4].
With the exception of the last point, we report in this paper significant progress in the development and application of these techniques leading to new physics interpretation. Much of this progress has occurred through the synergetic combination of experimental, theoretical and numerical simulation results. The outcome is an interesting picture of the interlink between E_r (static and fluctuating) and the mean profiles (n_e, T_e etc.) and the density turbulence, and thus with confinement.

2. Doppler reflectometry technique

2.1. Reflectometer hardware

FIG. 1(a) shows a schematic of the Doppler reflectometer diagnostic on ASDEX Upgrade (AUG). Microwave power ($50 - 75$ GHz) is launched at an angle to the density gradient from the tokamak low-field-side in either O or X-mode polarization. An adjacent antenna collects the scattered/reflected signal which is down-converted using a heterodyne receiver with in-phase and quadrature detection. The complex amplitude signals ($I + iQ = Ae^{i\phi}$) are sampled at 20 MHz for upto 7 seconds [1,2]. The antenna angle (poloidal) at the plasma boundary θ_o, *FIG. 1(b)*, makes the reflectometer sensitive (via Bragg) to a specific non-zero turbulence wavenumber $k_\perp = 2k_i = 2Nk_o$ where N is the refractive index and $k_o = \omega_o/c$ the probing wavenumber [4]. For nearly flat cutoff layers $N^2 \approx \sin^2\theta_o$ and thus $k_\perp \approx 2k_o \sin\theta_o$ for the $m = -1, -2, ..$ Bragg orders [8]. If the turbulence is moving then a Doppler frequency shift $\omega_D = \vec{u}\cdot\vec{k} \approx u_\perp k_\perp$ (for $k_\perp \gg k_\parallel$) is induced in the measured spectra, which is directly proportional to the perpendicular rotation velocity $u_\perp = v_{E\times B} + v_{ph}$ of the turbulence moving in the plasma. The direct reflection component $m = 0$ (normal reflectometry) is minimized by careful design of the antenna radiation pattern so as to optimise the Doppler spectral peak.

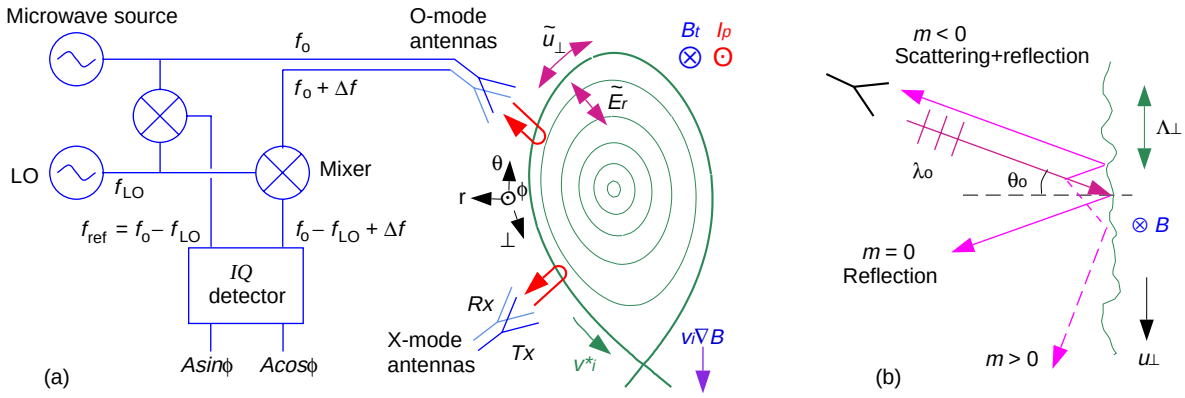

FIG. 1: (a) Schematic of Doppler reflectometer on AUG, (b) Doppler geometry showing scattered plus reflected orders.

2.2. Turbulence phase velocity

If the turbulence phase velocity v_{ph} is known, or small $v_{E\times B} \gg v_{ph}$, then $E \times B$ velocity, and hence the radial electric field E_r, can be extracted directly from the Doppler shift with good accuracy. Linear and non-linear turbulence simulations indicate that $v_{ph} \sim \pm\mathcal{O}(3)\rho_s c_s/R$ for ion-temperature gradient (ITG) and trapped electron mode (TEM) type turbulence [9], which is of the order of a few hundred metres per second for AUG core conditions. In the tokamak edge the dominant toroidal electron drift wave (EDW) turbulence is more non-linear. Nevertheless GS2 gyro-kinetic simulations indicate $v_{ph} \ll \rho_s c_s/L_n \rightarrow 0$ at typical probed $k_\perp > 6$ cm^{-1} particularly when the density and temperature scale lengths are comparable, e.g. $\eta_{e,i} = L_n/L_{T(e,i)} \sim \mathcal{O}(2)$.

2.3. Turbulence amplitude

An important factor is the turbulence amplitude at the probed wavenumber. Reflectometer simulations [10] and measurements [1] show that at low fluctuation amplitudes the $m = -1$ spectral peak will be lost in the wings of a dominant $m = 0$ peak or beneath the diagnostic noise floor. Turbulence k-spectrum measurements and numerical simulations indicate that for ITG turbulence the spectrum peaks around $k_\perp\rho_s \sim 0.3$ while for EDW the sharp spectral roll-off is higher at $k_\perp\rho_s \sim 1$. Since $\rho_s = c_s/\omega_{ci}$ depends on the machine parameters this defines the practical range of probable $k_\perp$, i.e. the antenna tilt angles.

2.4. Analysis technique

The Doppler shift frequency is obtained by fitting multiple Gaussians to the asymmetric component of the complex amplitude spectra - c.f. *FIG. 2* - averaged over $3-20$ ms. By stepping the microwave probe frequency staircase fashion a radial profile can be measured in $100-200$ ms with typically 20 steps or more. The profile repetition period is set by the desired radial resolution (number of steps) and the Doppler resolution (step length). The measurement (cutoff) position and the N^2 are obtained using the TORBEAM beam tracing code [11] for each measurement with flux surface reconstructions from the CLISTE equilibrium code and a spline fitted density profile using DCN interferometry, Thomson scattering, edge Lithium beam and FM profile reflectometry data when available.

3. Radial Electric field profiles ($v_{E\times B} \gg v_{ph}$)

In the tokamak scrape-off-layer the $u_\perp$ velocity always flows in the ion drift direction, i.e. a $+E_r$, but reverses across the separatrix primarily due to the pedestal pressure gradient to form a deep negative E_r well [1,3]. *FIG. 2* shows a typical E_r profile for a -2 T / $+1$ MA ELMy H-mode with 12 MW of NBI heating ($v_{E\times B} \gg v_{ph}$) together with example Doppler spectra.

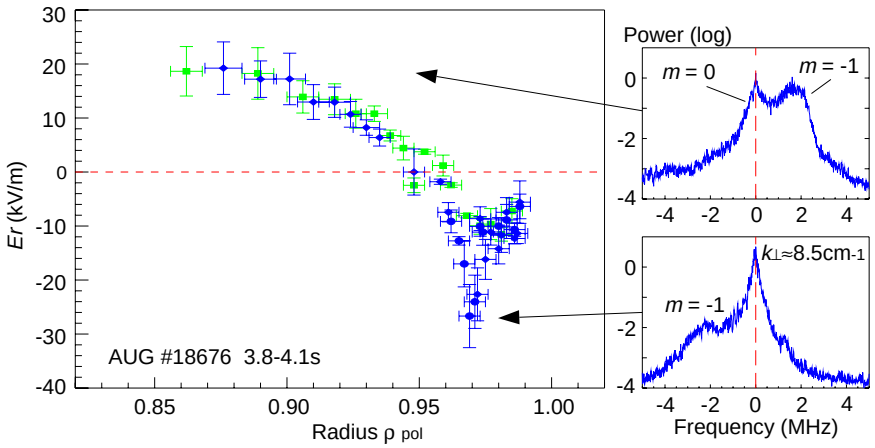

FIG. 2: E_r profile for H-mode #18676 with reflectometer spectra showing $m=0$ and $m=-1$ Doppler peaks.

The strength of the E_r well increases directly with confinement, with typically -5 kV m^{-1} for ohmic and L-mode conditions, jumping to around -30 kV m^{-1} for H-mode and in excess of -50 kV m^{-1} for improved H-modes [5]. The deepest E_r wells have so far been obtained in Quiescent H-modes [1,12]. Such large E_r values are possibly linked to the absence of ELMs in the QH-mode. By holding the microwave probing frequency constant across the L to H-mode transition gives sub-ms time resolved measurements showing the E_r evolution occurs in concert with the pressure gradient increase ∇P, but is preceeded $\sim 1-5$ ms by a drop in $\tilde{n}_e$ (proportional to the Doppler amplitude fluctuations) in the shear region [2]. Generally, the change in $u_\perp$ appears to be matched by the change in the electron diamagnetic drift velocity v_e^*.

3.1. ELMs

H-mode Doppler measurements are notably difficult due to (a) the reduced fluctuation level which often results in no usable Doppler signal, and (b) the presence of perturbative ELMs which produce fast radial cutoff layer movements. Nevertheless, fast time resolved measurements clearly show the E_r well collapsing in concert with the edge pedestal during type-I ELM events. However, a side benefit of ELMs is the localized edge turbulence build-up prior to each ELM which often provides the only means of generating a measurable Doppler signal in an otherwise quiescent region [1].

4. Doppler correlation reflectometry

4.1. E_r shear

Confinement theories suggest that the strength and sign of the E_r shear may be the more important parameter rather than the E_r magnitude alone. By adding a second Doppler channel

launching through the same antennas but with a fixed small frequency difference the instantaneous E_r shear profile can be measured [5]. *FIG. 3(a)* shows radial profiles of the instantaneous E_r shear during L (1.4 MW) and H-mode (4 MW NBI) phases of #19151. Corresponding to the flanks of the E_r well there is a positive peak associated with the separatrix and a negative peak associated with the pedestal region. The shear is practically zero elsewhere. The positive peak stays roughly constant and only the negative peak rises and with the L-H transition [5]. The negative shear width is constant at around 5 cm. The preeminence of the negative shear dependence is consistent with Biglari-Diamond-Terry model for the L-H transition [13]. Once the H-mode is formed the E_r well is insensitive to additional heating power. Plasma triangularity scans also confirm that the E_r well increases with triangularity and plasma confinement (e.g. H_{98} factor and confinement time). Configuration ramps from upper single null through double null to a lower single null also show the well is reduced during upper X-point when the ion ∇B drift is away from the divertor. Extensive modelling of these edge and SOL E_r profiles has been performed using the B2SOLPS5.0 transport fluid code to investigate the role of parallel flows. The simulations generally recreate the shape and magnitude of the experimental E_r profile [14].

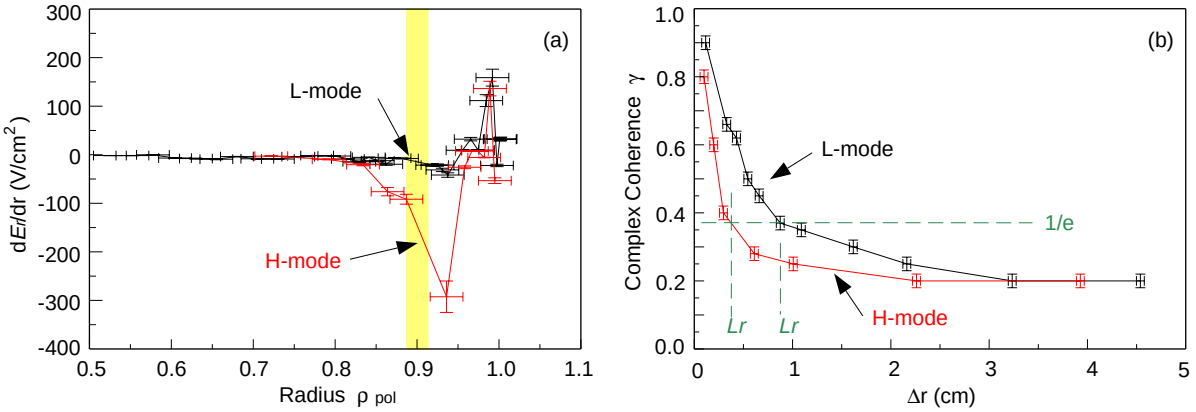

FIG. 3: (a) Instantaneous E_r shear and, (b) radial correlation profiles for L and H-mode phases of #19151. Shaded box shows measurement location of L_r.

4.2. Turbulence radial correlation lengths

By switching the launch frequency pattern of the two Doppler reflectometer channels from a fixed-frequency difference to a stepped-frequency difference, a measure of the radial correlation length L_r of the turbulence can also be obtained together with the E_r profile. *FIG. 3(b)* shows the coherence γ vs radial separation Δr in the negative shear zone ($\rho_{\rm pol} \sim 0.9$) for the corresponding L and H-mode phases of *FIG. 3(a)*. L_r (defined as $\gamma(L_r) = 1/e$) drops to less than 0.5 cm in the H-mode, coinciding with the increased E_r shear. Moving inward sees the L-mode L_r increasing, reaching 2 cm or so at mid-radius [15]. Since the use of Doppler reflectometry for correlation measurements is a new technique, extensive modelling studies using a 2D finite-difference time-domain full-wave code have been performed. The simulations show that the L_r obtained from the $m = -1$ Doppler peak scales correctly with the modelled $\tilde{n}_e$ correlation length - i.e. inversely with k_r. There is a slight sensitivity to the poloidal k spectrum (increases with wider k_p) and the Doppler tilt angle (decreases with $k_\perp$). However, the most promising aspect, which is contrary to $m = 0$ normal incidence correlation reflectometry, is the insensitivity to the turbulence amplitude $\tilde{n}_e$. Using the simulation results allows the interpretation of experimental data using tilt angle variation to show that L_r decreases with increasing average plasma triangularity, i.e. consistent with improving confinement observed with increasing δ_{av} [16].

5. Turbulence transitions ($v_{E\times B} \sim v_{ph}$)

5.1. Collisionality dependence

Changes in the behaviour of density peaking and the response in the electron heat flux with variations in the collisionality have been attributed to transitions in the core turbulence from TEM to ITG dominated [17,18]. This hypothesis can be tested by measuring changes directly in the turbulence velocity using Doppler reflectometry. In the tokamak core the $u_\perp$ magnitude and direction depends on the plasma scenario, particularly on the momentum driven rotation by neutral beam injection. However, in non-NBI heated discharges $u_\perp$ drops to a few $\mathrm{km\,s^{-1}}$ which is comparable to the expected turbulence phase and poloidal fluid velocities, i.e. $v_{E\times B} \sim v_{ph}$. *FIG. 4* shows $u_\perp$ radial profiles for lower single-null ohmic shots with various n_e and I_p. The profiles show the usual edge positive and negative peak structure associated with the SOL and ∇P regions - which is notably robust due to high collisionality (above banana limit) which appears to affect the dominant drift wave turbulence only marginally. However, the core $u_\perp$ reverses from the ion to the electron drift direction with increasing collisionality $\nu^*(=\nu_{ei}/\omega_{be}\epsilon)$ [6].

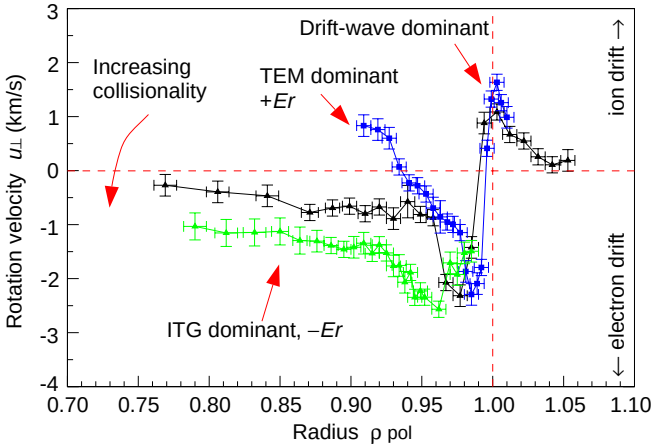

FIG. 4: Ohmic $u_\perp$ profiles for increasing ν^*.

5.2. Phase velocity calculations

In *FIG. 5* a variation in ν^* over almost two orders of magnitude via ohmic density and I_p scans shows a smooth reversal in $u_\perp$ at $\rho_{\mathrm{pol}} \approx 0.7$. Matched simulations were made for these discharges using the GS2 linear gyro-kinetic code. Plotted in *FIG. 5* is the phase velocity $v_{ph} = \omega_r/k_\theta$ (points and fit) computed from the real part of the dominant instability frequency corresponding to the poloidal wavenumber at which the growth rate $\gamma/k_\perp^2$ is maximum at $\rho_{\mathrm{pol}} = 0.6 - 0.7$. It shows an abrupt transition in the dominant core turbulence between TEM to ITG with a corresponding phase velocity reversal from the electron to ion drift directions. For this data the probed $k_\perp = 10 - 12\ \mathrm{cm}^{-1}$, i.e. $k_\perp \rho_s \sim 0.4$ which covers both the ITG and TEM expected wavelength range. The magnitude of the Δv_{ph} across the transition matches the jump in the $u_\perp$ from low to high collisionality. This suggests a smooth linear variation in the resultant $v_{E\times B} = u_\perp - v_{ph}$ against $\log \nu^*$ (i.e. exponential in ν^*), and hence a core E_r which changes sign with the dominant turbulence. (Note this is a new interpretation compared to the straight line $u_\perp$ fit used earlier [6] which allows for a more complete reconciliation of all data.) At high collisionality, TEM turbulence is predicted to be linearly stable, leaving the predominant ITG. At low collisionality TEM dominates, however, in between simulations predict similar growth rates for TEM and ITG, creating a transition region with mixed turbulence nature. The $u_\perp$ curve suggests that the density structures drift with a resultant velocity between TEM

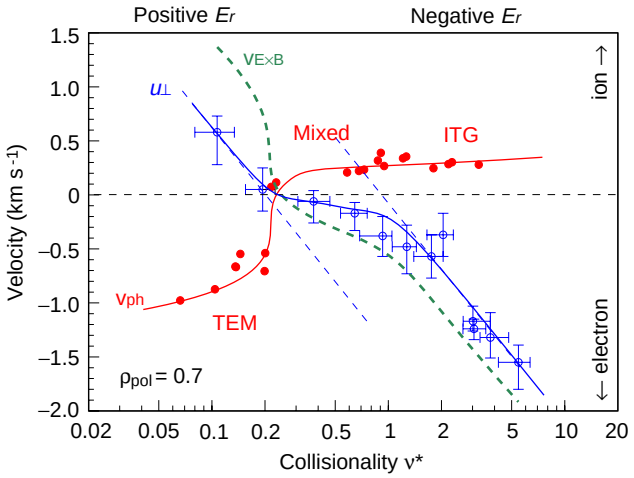

FIG. 5: $u_\perp$ and v_{ph} at $\rho_{\mathrm{pol}} \approx 0.7$ vs collisionality ν^* from ohmic shots with different $\bar{n}_e$ and I_p.

and ITG. Note that the GS2 code tracks the dominant mode and does not resolve sub-modes - which may explain the bump in the $v_{E\times B}$ curve (dashed-line) in *FIG. 5*. Attempts to identify two separate modes in the Doppler spectrum corresponding to $v_{E\times B} + v_{ph\,(ITG/TEM)}$ (so-called peak-splitting) have not revealed convincing double peaks or discernable modulation in $u_\perp$. This may be partly due to the diagnostic resolution, however, initial reflectometer simulations indicate the spectral resolution should be sufficient for this application.
In addition to density scans (within and from shot-to-shot) the collisionality can be perturbed via the electron temperature by applying upto 800 kW of on-axis electron cyclotron heating in various power steps. Similar $u_\perp$ behaviour to *FIG. 5* is obtained, although the transition from ITG to TEM tends to be sharper. Also, at high densities (the ITG range) the turbulence spectra are significantly wider - beyond that due to rotational broadening alone, suggesting a change in the underlying turbulence k-spectrum.

5.3. Fluid velocities

Combining the interpreted $v_{E\times B}$ with measured diamagnetic velocities allows the perpendicular ion fluid velocity $v_{\perp i} = v_{E\times B} + v_i^*$ to be deduced. At low collisionalities $v_{i\perp} \approx +4.8\,\mathrm{km\,s^{-1}}$ (ion drift direction) falling to $-0.7\,\mathrm{km\,s^{-1}}$ (electron) at high ν^*. Since $v_{\perp i} = v_{\phi i}\,B_\theta/B - v_{\theta i}\,B_\phi/B$ this implies either, that poloidal fluid velocities of $v_{\theta\mathrm{i}} \approx -v_{\perp\mathrm{i}}$ are required with values of a factor of 10 larger than neoclassical predictions, or exceedingly large toroidal fluid velocities. For example, at the low ν^* range if $v_{\theta i}$ is neoclassical then $v_{\phi i}$ would need to be in excess of $+30\,\mathrm{km\,s^{-1}}$ (co-I_p). Such large toroidal rotations are not supported by CXRS measurements on NBI beam-blips in ECRH shots [6].

6. Zonal flows and GAM ($v_{E\times B}$ fluctuations)

6.1. $u_\perp$ fluctuation measurements

Of major importance to confinement are zonal flows and associated geodesic acoustic modes (GAM) - radially localized oscillating $E \times B$ flows with an $m = n = 0$ mode structure but finite radial extent $k_r \neq 0$ - which theory predicts are generated by non-linear turbulence interactions and are found to moderate the turbulence amplitude via shear de-correlation [19]. Since $u_\perp$ contains the $E \times B$ velocity, fluctuations in E_r will translate directly to f_D, i.e. Doppler reflectometry can be used to directly measure $\tilde{E}_r$ with high spatial and temporal resolution. f_D will also register fluctuations in B, v_{ph} or θ_o. However, $\tilde{v}_{ph} = 0$ as this requires a non-obvious non-linear effect. While B and θ_o modulation due to MHD can be detected as cutoff layer tilting modulates the reflected signal power which can be measured separately [7].

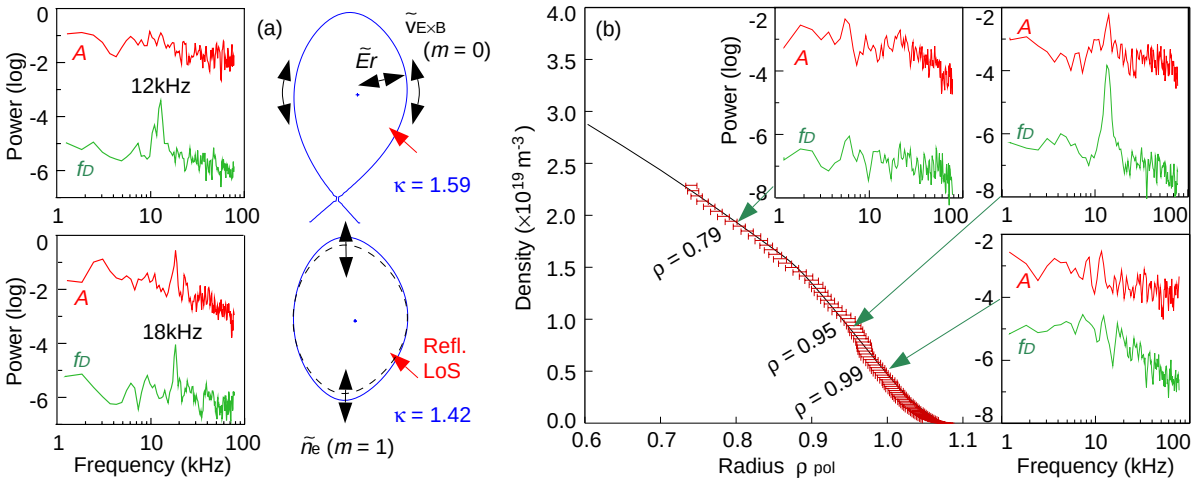

FIG. 6: (a) Edge GAM spectra for ohmic divertor and limiter geometry #20737, and (b) at 3 radial locations in $\kappa = 1.12$, $q_{95} = 3.5$ ohmic #20787. n_e profile is from FM reflectometry.

6.2. GAM localization

By using a sliding FFT a time sequence of f_D and amplitude A fluctuations can be generated from the complex amplitude spectra $S(f)$. The weighted spectral mean gives the instantaneous $f_D = \sum f.S(f) / \sum S(f)$ while the integrated spectra $A = \sum S(f)$ gives a measure of $\tilde{n}_e$ at the selected $k_\perp$. *FIG. 6* shows a series of f_D and A spectra at (a) the edge in divertor and limiter phases of an ohmic discharge #20787 and (b) at three radial locations in an almost circular $\kappa = 1.12$ ohmic shot #20787. Strong coherent oscillations are observed in f_D between $5 - 25$ kHz - even in the absence of MHD activity - with an amplitude of 2 to 3 orders of magnitude above the background. The peaks appear in the edge density gradient region - where the turbulence vorticity and E_r shear are largest [7]. No coherent activity is seen in the open-field SOL region (f^{-1} spectra), nor inside of the density pedestal region, i.e. core (flat spectra). The mode has the features expected of a GAM, its frequency scales linearly with $(T_e + T_i)^{1/2}$ over a wide range of ohmic and L-mode conditions. So far GAMs have not been observed in H-modes. There is no peak dependence on B or n_e. There is no measurable magnetic perturbation, and, for diverted plasmas there is practically no density perturbation, i.e. A peak. In X-mode the Doppler reflectometer measures from slightly below the magnetic axis, as shown by the red arrows in *FIG. 6(a)*, which for highly elongated diverted plasmas generally means the diagnostic is insensitive to the GAM's $m = 1$ pressure side-band mode structure. Only for low elongation (non-diverted) plasmas does a corresponding A peak appear where the reflectometer line-of-sight is closer to the $m = 1$ mode maxima. The precise mode structure is still to be confirmed with poloidal measurements.

6.3. GAM parameter dependence

The mode frequency scales as $\omega = Gc_s/R$ (sound speed over major radius), as shown in *FIG. 7* for a range of ohmic Deuterium discharges. The scale factor $G \sim \mathcal{O}(1)$ also shows the appropriate variation with ion mass for Hydrogen, Deuterium and Helium plasmas, but with a strong inverse dependence on the plasma elongation κ and a weak direct dependence on the local q. A series of dedicated κ and q scans have been performed resulting in a best-fit scaling:

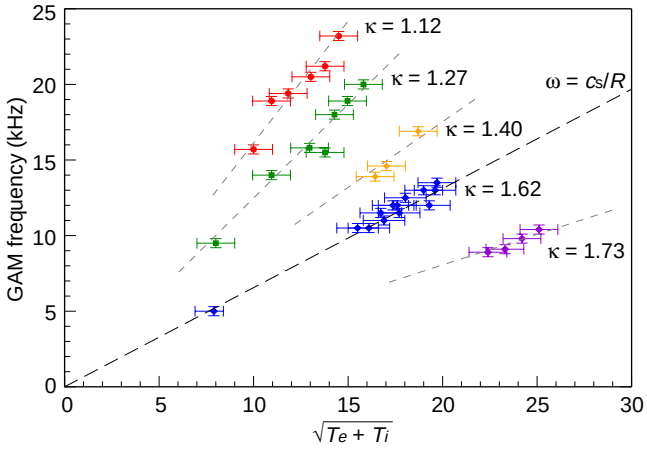

FIG. 7: GAM frequency vs $(T_e+T_i)^{1/2}$ for increasing plasma elongation κ at fixed $q_{95} = 3.85$.

$$\omega_{GAM} \approx \frac{c_s\, S}{R}\left(\frac{1}{1+\kappa} - \frac{1}{q}\right) \qquad (1)$$

where $c_s^2 = (T_e + T_i)/M$ and $S \approx 4\pi$. There is some radial variation in the factor S which indicates further parameter dependence. In general ω_{GAM} is not a smooth monotonic function of radius but shows distinct plateaus a few cm wide which suggests several zonal flow layers. Radially the GAM reaches into as far as the density pedestal, typically $\rho_{\rm pol} > 0.92$, but at high q_{95} and low κ the n_e pedestal is less pronounced and the GAM peak can be seen as far in as $\rho_{\rm pol} \sim 0.75$. This points to a link with high turbulence drive, large vorticity and E_r shear. The link between the GAM/zonal flows and turbulence moderation is also demonstrated by a counter modulation in the density and broadband E_r fluctuations with the GAM peak intensity. The q dependence in eqn. 1 predicts a limit for lowest q for which the GAM can exist. Experimentally this is observed in the low κ discharges where as the q profile falls the innermost GAM position is pushed progressively outward. Finally, GAMs also disappear at high collisionality.

7. Summary and discussion

Doppler reflectometry is a simple diagnostic technique capable of measuring the E_r profile, its shear and its fluctuations with high spatial and/or temporal resolution. With a two reflectometer channel configuration launching with the same line-of-sight, the local turbulence amplitude $\tilde{n}_e$, correlation length L_r and E_r shear can be obtained together from one diagnostic.

The measurements presented here show that the magnitude and width of the edge negative E_r shear region is the dominant factor in the improved confinement of the H-mode. The increased shear coincides with both reduced turbulence amplitude and L_r. The ability of normal-incidence correlation reflectometry to correctly measure L_r from the $m = 0$ direct reflection component is still being debated. However, full-wave simulations are indicating that the $m \neq 0$ component measured by the Doppler correlation technique gives a more robust L_r value.

Fluctuations in $v_{E\times B}$ with transverse wavelengths greater than the reflectometer spot size (a few cm) translate directly to the Doppler shift. Observations show a coherent oscillation in edge high vorticity/shear region with all the features of a GAM. Its frequency scales with c_s/R but with an inverse dependence on elongation κ and direct variation with local q. The $m = n = 0$ mode structure is still to be confirmed but there is evidence of the $m = 1$ pressure side-band. GAMs are only seen in ohmic and L-mode, not in H-mode, possibly due to the lower turbulence level, i.e. reduced zonal flow drive, or due to the high rotation shear in the edge. The GAM frequency is not a smooth function of radius but shows plateaus, suggesting multiple zonal flow layers with radial extents of a few cm. Radially, the GAM is also bounded by both the density pedestal and by the q profile. Specifically, dropping the q profile reduces the GAM inner radial reach. While GAMs are not observed in the core there is still the possibility of the low frequency zonal flow branch.

In the absence of large $E \times B$ flows the effect of the turbulence phase velocity becomes evident. Clear evidence of the transition between TEM and ITG turbulence has been obtained from the core of ohmic and ECRH L-mode discharges. Further, the measured $\Delta u_\perp$ matches the Δv_{ph} jump predicted by the GS2 linear gyro-kinetic code - which essentially validates the code for these conditions. In the transition zone between ITG and TEM, simulations predict equable growth rates. However, there is no evidence of 'line-splitting' (i.e. two spectral peaks) in the data so far, plus the smooth $u_\perp$ variation suggests that the density fluctuations/structures take a mean velocity between that of TEM/ITG.

References

[1] CONWAY, G.D. et al., Plasma Phys. Control. Fusion **46** (2004) 951.
[2] KLENGE, S., Ph.D. Thesis, Univ. Stuttgart (2005) Sierke Verlag, ISBN 3-933893-36-4.
[3] HIRSCH, M. et al., Plasma Phys. Control. Fusion **48** (2006) S155.
[4] HENNEQUIN, P. et al., Nucl. Fusion **46** (2006) S771.
[5] SCHIRMER, J. et al., Nucl. Fusion **46** (2006) S780.
[6] CONWAY, G.D. et al., Nucl. Fusion **46** (2006) S799.
[7] CONWAY, G.D. et al., Plasma Phys. Control. Fusion **47** (2005) 1165.
[8] HIRSCH, M. et al., Plasma Phys. Control. Fusion **43** (2001) 1641.
[9] BEER, M., Ph.D. Thesis Princeton Univ. (1995).
[10] CONWAY, G.D., Plasma Phys. Control. Fusion **41** (1999) 65.
[11] POLI, E. et al., Comput. Phys. Commun. **136** (2001) 90.
[12] SUTTROP, W. et al., Nucl. Fusion **45** (2005) 721.
[13] BIGLARI, H. et al., Phys. Fluids **B2** (1990) 1.
[14] ROZHANSKY, V. et al., Plasma Phys. Control. Fusion **48** (2006) 1425.
[15] SCHIRMER, J. Ph.D. Thesis, Ludwig-Maximilians Univ., Munich (2005).
[16] SCHIRMER, J. et al., 33rd EPS Conf.(Rome) (2006) P2-136
[17] ANGIONI, C. et al., Phys. Plasma **12** (2005) 040701.
[18] RYTER, F. et al., Phys. Rev. Lett. **95** (2005) 085001.
[19] DIAMOND, P.H. et al., Plasma Phys. Control. Fusion **47** (2005) R35.